Electromagnetically induced transparency and slow light in an array of metallic nanoparticles

Vassilios Yannopapas,[1,2,*] Emmanuel Paspalakis,[1] and Nikolay V. Vitanov[2,3]
[1]*Department of Materials Science, University of Patras, GR-26504 Patras, Greece*
[2]*Department of Physics, Sofia University, James Bourchier 5 Boulevard, 1164 Sofia, Bulgaria*
[3]*Institute of Solid State Physics, Bulgarian Academy of Sciences, Tsarigradsko Chaussée 72, 1784 Sofia, Bulgaria*
(Received 7 March 2009; published 1 July 2009)

We present a classical analog of electromagnetically induced transparency occurring when light is absorbed by a two-dimensional lattice of metallic spheres mounted on an asymmetric dielectric waveguide. The transparency is manifested as a spectral hole within the surface-plasmon absorption peak of the metallic spheres and is a result of destructive interference of the waveguide modes with incident radiation. The presence of transparency windows is accompanied by slow light effect wherein the group velocity is reduced by a factor of 6000. At the same time, the minimum length for storing a bit of information is of the order of 100 nm. The proposed setup is a much easier means to achieve transparency and slow light compared to existing atomic, solid-state, and photonic systems and allows for the realization of ultracompact optical delay lines and buffers.

DOI: 10.1103/PhysRevB.80.035104 PACS number(s): 73.20.Mf, 42.50.Gy, 42.25.Bs, 78.67.Bf

I. INTRODUCTION

Electromagnetically induced transparency (EIT) (Ref. 1) is one of the most fascinating effects of quantum optics as it allows the coherent control of the optical properties of materials and processes. In this phenomenon, an otherwise opaque medium of three-level atoms becomes transparent to a resonant probe-laser field that couples one of the transitions by the application of a strong dressing laser field to the other transition. EIT has been observed in atoms,[2] rare-earth-ion-doped crystals,[3] semiconductor quantum wells,[4] quantum dots,[5] and Bose-Einstein condensates[6] (for a review see Ref. 7). Recently, there has been an increasing interest in classical-light analogs[8] to quantum EIT, mainly based on optical microresonators.[9] Possibly, the main technological applications of EIT are due to the accompanying slow light phenomenon which, among other things, allows for the realization of delay lines and buffers in optical circuits.

In pursuit of more compact optical components, the field of plasmonics, i.e., the interaction of light with metallic nanostructures via the excitation of surface waves known as surface plasmons (SPs), has been a blueprint for future nanosized, all-optical circuitry thanks to the strong localization of light in subwavelength volumes.[10] In this respect, the miniaturization of optical delay lines and buffers by using SP-based EIT is a particularly appealing idea. To this end, metamaterials of elaborate metallic components have been predicted recently[11,12] to exhibit EIT in the THz regime. Also, millimeter-scale metallic metamaterials have been experimentally shown to exhibit EIT in the GHz regime.[13]

In this paper, we propose a less involved structure exhibiting EIT within the *visible* regime. It is depicted in Fig. 1 and consists of a rectangular lattice of gold spheres on top of an indium-tin-oxide (ITO) substrate. The EIT phenomenon emerges when the ITO substrate supports guided modes which are simultaneously excited with the SPs of the gold spheres. This[14] and similar structures[15] have already been realized experimentally as a means to tailor light extinction from metal nanoparticles by the use of a guiding substrate. However, the analogy with the EIT phenomenon and its profound applications in optoelectronics had not been spotlighted at the time. By employing multiple-scattering electrodynamic calculations we show that it is possible to achieve EIT with the above structure, in which case the speed of light can be reduced by a factor of the order of 10^4 relative to the speed in vacuum. Furthermore, we find that, at the transparency maximum, the dielectric function and the corresponding refractive index are both zero rather than unity as in traditional quantum EIT.

II. EIT SCHEME

An EIT scheme requires a bright and dark state corresponding to the same frequency. The bright state couples strongly with incident light and, as such, it exhibits a wide absorption band. The dark state couples weakly with external light and possesses a significantly longer lifetime (high-quality factor). In the system studied here, the bright state is represented by the highly absorptive SP state of a two-dimensional (2D) lattice of metallic (gold) spherical nanoparticles. In reality, due to the periodicity of the lattice, one must speak of a SP band which arises from the interaction of SP states of neighboring nanoparticles. However, the dispersion of the SP band with the wave-vector **k** is small and one can approximate it with a SP state for our purposes. The dark state is provided by a dielectric (ITO) waveguide when a

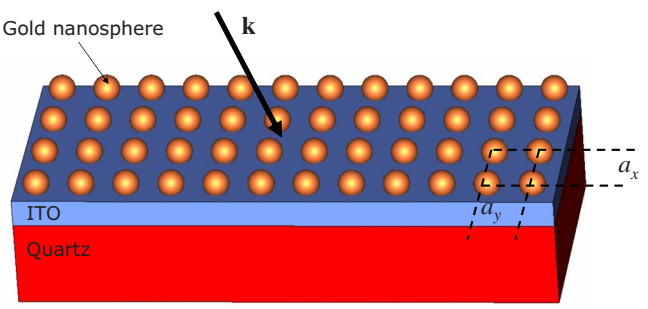

FIG. 1. (Color online) Computational setup for the classical EIT we propose here.

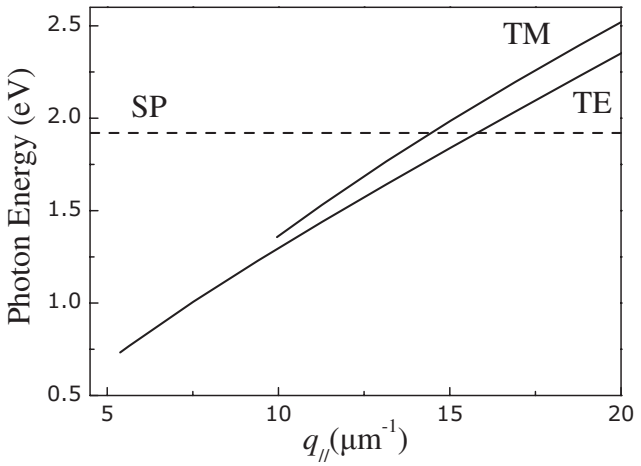

FIG. 2. Solid lines: dispersion curves of the TE and TH waveguide modes for an ITO film, 140 nm thick, sandwiched between air and quartz. Broken line: energy of the surface-plasmon peak of a rectangular array of gold spheres.

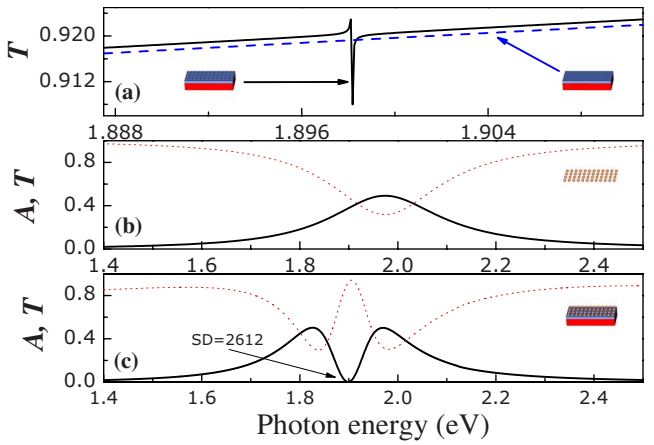

FIG. 3. (Color online) Absorbance A and transmittance T spectra for light incident *normally* and polarized along the y axis for various structures. (a) Broken line: transmittance spectrum for an ITO (ϵ=3.8) waveguide of thickness 140 nm sandwiched between air (ϵ=1) and quartz (ϵ=2.1). Solid line: transmittance for the same ITO waveguide but with a perturbative rectangular lattice (a_x =403 nm and a_y=300 nm) of almost transparent dielectric spheres (ϵ_s=1.1 and S=50 nm) sitting on top of it. (b) Absorbance (solid line) and absorbance (dotted line) spectra for the same rectangular lattice as in (a) whose sites are occupied by gold nanospheres. (c) The same spectra for the lattice of gold nanospheres of (b) mounted on top of the ITO waveguide of (a).

periodic lattice is inscribed on its surface. The latter effect can be understood as follows.

III. RESULTS AND DISCUSSION

A homogeneous dielectric plate sandwiched between two semi-infinite media with refractive indices smaller than that of the plate supports, besides the scattering states, also TE and TH waveguide modes which correspond to dispersion relations as in Fig. 2. Along any direction parallel to the plate these modes have the form of propagating waves with a wave-vector $\mathbf{q}_\parallel$. Along the normal direction they decay exponentially away from the plate on either side of it and they are therefore considered as bound EM states. This means that they cannot match continuously a propagating mode of the EM field outside the film as momentum and energy cannot be conserved simultaneously. When we put a 2D periodic lattice of particles on the film, waveguide modes can be transformed from bound to radiative through an umklapp process: a plane wave of wave-number q, incident on the periodic array, generates a number of diffracted beams with wave vectors given by $\mathbf{K}_\mathbf{g}^{\pm}=\mathbf{k}_\parallel+\mathbf{g}\pm[q^2-(\mathbf{k}_\parallel+\mathbf{g})^2]^{1/2}\hat{z}$ where $\mathbf{g}$ stands for the reciprocal-lattice vectors of the rectangular lattice and $\mathbf{k}_\parallel$ is the parallel wavevector reduced within the surface Brillouin zone (SBZ) of the lattice. If $q<|\mathbf{k}_\parallel+\mathbf{g}|$ we obtain evanescent diffracted beams which can match continuously the corresponding guided waves of the same polarization and of the same $\mathbf{q}_\parallel=\mathbf{k}_\parallel+\mathbf{g}$, provided they have the right frequency. From another point of view, because of the 2D periodicity of the coating layer, the waveguide frequency bands are folded within the SBZ of the given lattice and acquire a small imaginary part due to the mixing with the extended (scattering) states.[16,17] Accordingly, the waveguide modes are no longer bound within the film, but leak into the outer region becoming virtual bound states. These modes can be excited by an externally incident wave and manifest themselves as resonances in the transmission spectrum as in Fig. 3(a).

Namely, Fig. 3(a) shows the transmittance curves of light incident normally on a single 140 nm thick ITO waveguide (dashed curve) and on the same waveguide with an almost empty rectangular lattice (a_x=403 nm and a_y=300 nm) of dielectric spheres (ϵ_s=1.1 and S=50 nm) sitting on top of it (solid curve). For the ITO waveguide without the lattice, the corresponding transmittance curve is a monotonically increasing function while for the ITO waveguide with the almost empty lattice exhibits a strong resonant structure due to the excitation of the virtual bound state. We have chosen the value a_x=403 nm so that the TE virtual bound state of the ITO waveguide matches the central frequency of the SP resonance (bright state) along the y axis, with the correct parallel wave-vector $q_\parallel$=15.8 μm^{-1} (second intersection point of Fig. 2). For simplicity, we have chosen to exclude the TM modes from the EIT phenomenon by choosing a_y=300 nm so that the corresponding first reciprocal-lattice vector g_1 is different (larger) from $q_\parallel$=14.4 μm^{-1} (first intersection point of Fig. 2). The virtual bound state of Fig. 3(a) will serve as the dark state in our classical analog of EIT since it couples weakly with external light and possesses a very long lifetime (narrow linewidth).

Figure 3(b) shows the absorbance and transmittance curves for light incident normally on the same rectangular lattice as in Fig. 3(a) but whose sites are occupied by 50 nm gold spheres. The spheres are described by a Drude-type dielectric formula, i.e., $\epsilon(\omega)=1-\omega_p^2/[\omega(\omega+i\tau^{-1})]$ where ω_p is the plasma frequency and τ is the free-electron relaxation time. In order to best fit available experimental data,[14] we have chosen the values: $\hbar\omega_p$=3.71 eV and $\omega_p\tau$=20. The absorbance curve of Fig. 3(b) has been obtained by the layer-multiple scattering (LMS) method,[18] in the dipole approxi-

mation. It has a typical Lorentzian shape and results from the excitation of SP band emerging from the interaction of the SP resonances of neighboring gold spheres. As mentioned above, the SP resonance will be the bright state of our EIT proposal since it couples and absorbs light very efficiently while it possesses a shorter lifetime than the virtual bound state of the ITO waveguide.

When the rectangular lattice of gold spheres of Fig. 3(b) is placed on top of the ITO waveguide of Fig. 3(a), the resulting structure (depicted in Fig. 1) exhibits the transmittance and absorbance curves of Fig. 3(c). We observe a spectral hole in the absorbance curve (maximum of the corresponding transmittance curve) centered at the middle of the absorbance curve. The emergence of this transparency window can be understood as follows: when light with frequency equal to that of the virtual bound state is incident on the waveguide, it excites two counterpropagating waveguide modes (toward the two opposite directions of the x axis in the case of Fig. 3). The total electric field at the interface of the waveguide/plasmonic lattice is the sum of the direct incident wave plus the waveguide modes which are 180° out of phase with respect to the incident wave.[14] These two electric-field components interfere destructively resulting in a vanishing total electric field and, hence, zero electric force acting on the free electrons of the gold spheres. As the electrons cease to move (respond) to the applied electric field, the SP mode is suppressed since it emerges from the collective oscillation of the free electrons.

The occurrence of transparency on the basis of an EIT analog is expected to herald the prominence of slow light effects (see Refs. 19 and 20 for a review on the subject). The slowdown factor $SD \equiv c/v_g$ (c: speed of light in vacuum, v_g: group velocity inside the EIT medium) can be calculated by inspecting the profile of the spectral hole in Fig. 3(c). At the central frequency, it is provided by[20] $SD = n_{\mathrm{bac}} + c(\ln A_N - \ln A_{\mathrm{EIT}})/(\Delta\omega D)$, where D is the thickness of the plasmonic lattice +ITO waveguide, $\Delta\omega$ the full width at half maximum of the EIT spectral hole and $A_{\mathrm{EIT}}(A_N)$ is the absorbance in (without) the presence of the EIT phenomenon. We find $SD = 2612$ which is a high value achieved at room temperature and without the need of second (control) laser source as in traditional EIT in semiconductor systems.[20]

Other parameters which are important in an optoelectronic device are the (3 dB) operating bandwidth $B = (\Delta\omega/2\pi)\sqrt{\ln 2/(\ln A_N - \ln A_{\mathrm{EIT}})}$ and the delay-bandwidth product $\Delta\tau B = \sqrt{\ln 2(\ln A_N - \ln A_{\mathrm{EIT}})}$.[20] For the case of Fig. 3(c) they turn out to be $B = 2.815 \times 10^{-5}\omega_p = 0.159$ THz and $\Delta\tau B = 1.999$. Although the value of the bandwidth B is similar to that obtained with semiconductor EIT systems[20] the delay-bandwidth product $\Delta\tau B$ corresponds to a much smaller minimum length to store a bit $L_{\mathrm{bit}} = D/(\Delta\tau B) = 2.26c/\omega_p = 120.075$ nm. This value is about a factor of four smaller than the *ideal* value obtained via semiconductor-based EIT (Ref. 20) and allows for the realization of compact delay lines and buffers.

In traditional EIT systems, the phenomenon of transparency within an absorption band is also manifested in the permittivity as the latter becomes unity, with a negligible imaginary part at the central transparency frequency. Since we do not have a bulk system as in usual EIT systems, we retrieve the above effective-medium parameters by inverting Fresnel's equations.[21,22] The results are shown in Fig. 4 along with the corresponding transmittance curve. We find that both the effective permittivity ϵ_{eff} and permeability μ_{eff} vanish at the center of the spectral hole (maximum of transmittance) resulting in a vanishing effective refractive index n_{eff} as well. We note, however, that zero is a valid value for the refractive index since there have already been proposals of metamaterials with such a feature.[23] When both ϵ_{eff} and μ_{eff} vanish, the corresponding impedance equals unity[24,25] and the material is transparent similarly to our case. We note that the refractive index may vanish only due to the effective permittivity ϵ_{eff} in which case we have total reflectance due to infinite impedance. As a final note on Fig. 4(c), one observes that below the zero-index value, n_{eff} becomes negative with small imaginary part.

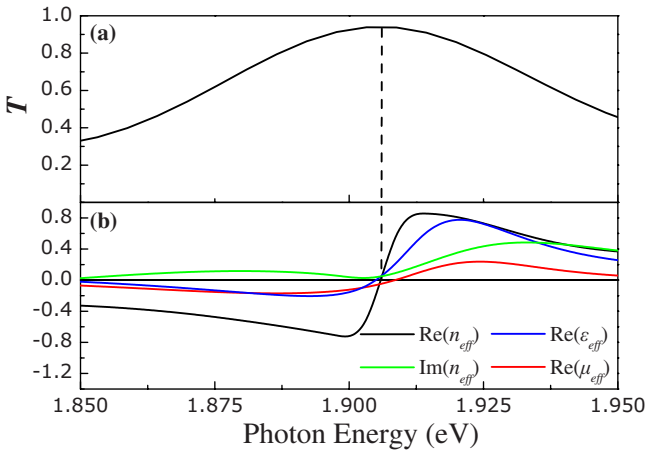

FIG. 4. (Color online) (a) A zoom-in around the transparency region of the transmittance spectrum of Fig. 3(a). (b) The corresponding effective-medium parameters ϵ_{eff}, μ_{eff}, and n_{eff}.

Next, in Fig. 5, we examine the absorbance curve for *almost normal* incidence, i.e., with small wavevector parallel

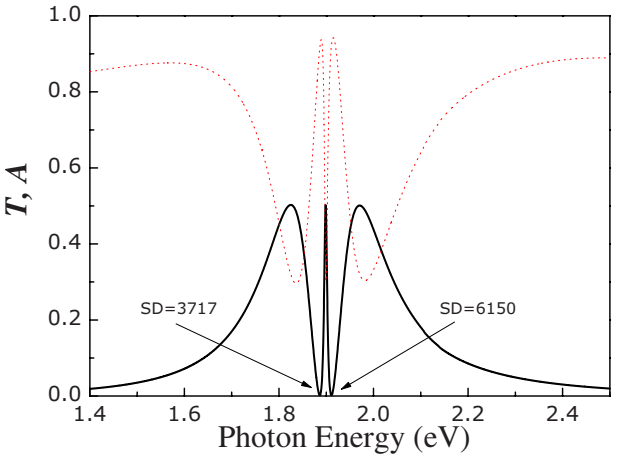

FIG. 5. (Color online) Absorbance (solid line) and transmittance (dotted line) spectra for light incident *almost normally* [$\mathbf{k}_{\parallel} = (0.015591, 0)$ $\mu\mathrm{m}^{-1}$ and polarization along the y direction] for the structure of Fig. 3(c) (rectangular lattice of gold nanospheres mounted on ITO waveguide).

to the surface, $\mathbf{k}_{\parallel}=(0.015591,0)\ \mu\mathrm{m}^{-1}$. The incident wave is *s* polarized and the electric field oscillates along the *y* axis as in Figs. 3 and 4. We observe that the absorbance curve exhibits two spectral holes (double transparency)[26] instead of one for normal incidence [Fig. 3(c)] corresponding to slow-down factors 3717 and 6150, respectively. The operating bandwidths are $B=0.105$ THz and 0.063 THz, respectively, while the delay-bandwidth products differ only about 1–2% from the case of Fig. 3(c) ($\Delta\tau B=1.999$). The occurrence of double transparency can be explained with group-theoretical arguments as follows.[17] In the absence of any lattice coating on a dielectric waveguide, the corresponding guided modes along one of the two axis [TE modes (*x* axis) or TM modes (*y* axis)] are doubly degenerate and, as stated above, they do not couple with normally incident light (bound states). In the presence of rectangular lattice on top of the waveguide, the degeneracy is lifted and two guided TE modes of different frequency emerge for each of the two opposite directions $\hat{x}$ and $-\hat{x}$, respectively. The low-frequency mode shares the same irreducible representation (Δ_4) of the point symmetry group (C_{2v}) of the wavevector with the externally incident light. As such, it couples with normally incident light, becoming, this way a virtual bound state. The high-frequency mode belongs to a different irreducible representation (Δ_2) and does not couple with normally incident light (bound state). This is why a single transparency window is evident in Fig. 3(c). For oblique incidence, the restrictions imposed by symmetry are relaxed and the high-frequency mode couples also with external light giving rise to the two transparency regions of Fig. 5.

Some remarks on the possible experimental measurements of the reported EIT system. As analyzed above, the double transparency region appears even for an infinitesimal parallel wavevector component in which case the Δ_2-symmetry mode starts leaking into free space and its corresponding lifetime becomes finite. In an actual experiment, the light beam incident on our EIT system is not literally a plane wave but a Gaussian beam having a finite waist *w*. The Fourier transform of the incident beam is $I(\mathbf{k}_{\parallel})\sim\exp(-\mathbf{k}_{\parallel}^2 w^2/8)$. Therefore, a normally incident Gaussian beam includes off-normal components ($\mathbf{k}_{\parallel}\neq 0$) as well and one is expected to observe two transparency dips in the absorbance spectrum as in Fig. 5. Of course, the wider the Gaussian beam is the fewer off-normal components contribute to the beam and the absorbance curve starts resembling that of Fig. 3(c). In order for the two cases of Figs. 3(c) and 5 to become also experimentally distinct, the minimum value of the waist *w* of the incident beam should be $w_{\min}\simeq 4/k_{\parallel}\simeq 0.256$ mm where $k_{\parallel}=0.015591\ \mu\mathrm{m}^{-1}$ (that of Fig. 5). The corresponding numerical aperture is $NA=2\lambda_0/(\pi w)\simeq 1.6\cdot 10^{-3}$ where λ_0 is the wavelength corresponding to the absorbance dip of Fig. 3(c).

Another point which would potentially influence the observation of the EIT effect in our proposal is that of disorder/imperfections in the lattice of gold nanospheres. In order to have an idea on the impact of the imperfections we next consider the case where the size of the nanospheres is not the same at each lattice site but assumes values according to a Gaussian distribution with mean radius 50 nm and variance σ^2. Figure 6 shows the absorbance curve for a normally incident plane wave on the same lattice for various values of σ, as obtained by the average *T*-matrix approximation (ATA) method. The ATA method, which has been originally introduced for the study of the electron properties of disordered metals and surfaces,[27,28] has been also employed for the study of the optical properties of random 2D (Ref. 29) and three-dimensional[30,31] arrays of spheres. In the ATA approach, the actual disordered crystal is replaced by an effectively periodic one whose lattice sites are occupied by same scatterers of an average *T*-matrix. From Fig. 6 it is evident that the transparency window and subsequently the slow-down factor are almost unaffected by the size disorder of the nanospheres even for unrealistically high values of σ, e.g., 10 nm. Of course, other types of disorder should also be considered such as positional disorder. However, an accurate accounting of positional disorder requires extensive, computationally intensive supercell calculations which will be dealt with in a future publication. We expect though, that if the mean position of the nanospheres coincides with a lattice site, the influence of positional disorder would be much similar to the effect of size disorder of Fig. 6.

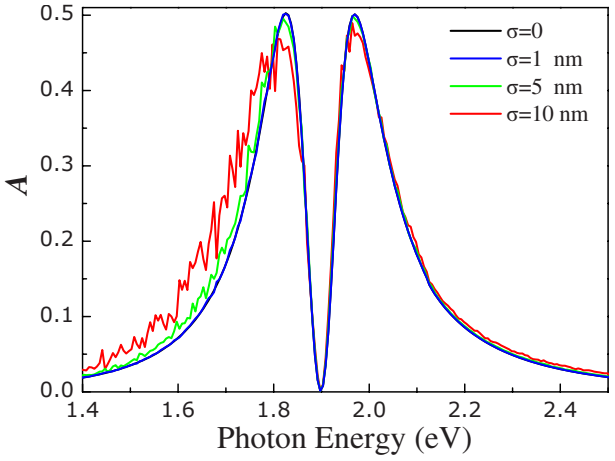

FIG. 6. (Color online) Absorbance spectra based on the ATA method for a lattice of gold nanospheres (the same lattice as in the previous figures) on top of an ITO waveguide where the radius of the spheres is random assuming values from a Gaussian probability distribution function with mean radius 50 nm and variance σ^2 (shown in the inset).

As also stated above, in all the calculations shown in this work, we have made use of a Drude-type dielectric function where ω_p and τ are taken from fitting to the experimental data of Ref. 14. Although the Drude model takes into account only the plasmonic excitations in a metal without taking into account inter and intraband transitions, it has been proven quite accurate around the region of a particle surface-plasmon peak as in our case.[32] So, the employment of an experimental dielectric function such as that of Johnson and Christy[33] would make no significant difference in the data shown.

A final remark on a potentially tunable operation of the proposed EIT system. Our proposal is distinct from the conventional atomic EIT systems as it does not require the combined action of two laser beams. It modifies the flow of light acting as a passive device without the need for a second

control laser beam. The action of a second laser which would allow for tuning of the transparency window is an option which cannot be seen with the proposed system since a possible shift of the EIT window with the action of a second laser (e.g., by shifting the position of surface-plasmon peak in case where the nanospheres were coated with a nonlinear material) should be accompanied by a corresponding modification of the underlying lattice period. Nevertheless, a certain degree of tunability can be achieved if the gold nanospheres are replaced by gold nanoshells, i.e., dielectric nanospheres coated with a metallic shell. In a metallic nanoshell, the position of the surface-plasmon resonances depends strongly on the thickness of the shell allowing for tuning of these frequencies according to a prescribed frequency.[32,34] However, the lattice constant of the underlying lattice should be consistently adjusted in order to achieve EIT. So, there is the possibility for tuning the transparency window to a specific spectral region but not dynamically since the lattice is fixed by the fabrication process.

IV. CONCLUSION

In conclusion, we have presented a classical analog to EIT which involves the interaction of a 2D lattice of gold spheres with a guiding ITO substrate. The observed transparency region corresponds to slowdown factors of the order of a few thousands. At the same time, the minimum length for storing a bit of information is of the order of 100 nm which is about a factor of four times smaller than in traditional semiconductor EIT schemes. This renders the structure ideally suited for ultracompact optical delay lines and buffers in future nanoscale optical circuits. The slowdown factors can be further improved by using a waveguide with a larger dielectric constant (and subsequent tuning of its thickness and lattice constant) which localizes the EM field more efficiently and results in a shorter lifetime of the corresponding virtual bound state. Another important feature of the present EIT phenomenon is the zero values assumed by the effective-medium parameters (permittivity, permeability, and refractive index), in agreement with the high transmittance associated with EIT. Finally, the observation of EIT and slow light is robust against disorder and numerical-aperture effects.

ACKNOWLEDGMENTS

This work has been supported by the European Commission's projects CAMEL, EMALI, and FASTQUAST, the Bulgarian NSF Grants No. 205/06, No. 301/07, No. 428/08, and the K. Karatheodory project B.699 of the University of Patras.

*vyannop@upatras.gr

[1] S. E. Harris, Phys. Today **50** (7), 36 (1997).
[2] K.-J. Boller, A. Imamoğlu, and S. E. Harris, Phys. Rev. Lett. **66**, 2593 (1991).
[3] B. S. Ham, P. R. Hemmer, and M. S. Shahriar, Opt. Commun. **144**, 227 (1997).
[4] G. B. Serapiglia, E. Paspalakis, C. Sirtori, K. L. Vodopyanov, and C. C. Phillips, Phys. Rev. Lett. **84**, 1019 (2000); M. C. Phillips, H. Wang, I. Rumyantsev, N. H. Kwong, R. Takayama, and R. Binder, *ibid.* **91**, 183602 (2003).
[5] S. Marcinkevicius, A. Gushterov, and J. P. Reithmaier, Appl. Phys. Lett. **92**, 041113 (2008); Z. Lu and K.-D. Zhu, J. Phys. B **42**, 015502 (2009).
[6] L. V. Hau, S. E. Harris, Z. Dutton, and C. H. Behroozi, Nature (London) **397**, 594 (1999).
[7] M. Fleischhauer, A. Imamoglu, and J. P. Marangos, Rev. Mod. Phys. **77**, 633 (2005).
[8] C. L. Garrido Alzar, M. A. G. Martinez, and P. Nussenzveig, Am. J. Phys. **70**, 37 (2002).
[9] S. Fan, W. Suh, and J. D. Joannopoulos, J. Opt. Soc. Am. A Opt. Image Sci. Vis. **20**, 569 (2003); L. Maleki, L. Maleki, A. B. Matsko, A. A. Savchenkov, and V. S. Ilchenko, Opt. Lett. **29**, 626 (2004); D. D. Smith, H. Chang, K. A. Fuller, A. T. Rosenberger, and R. W. Boyd, Phys. Rev. A **69**, 063804 (2004); M. F. Yanik, W. Suh, Z. Wang, and S. Fan, Phys. Rev. Lett. **93**, 233903 (2004); Q. Xu, S. Sandhu, M. L. Povinelli, J. Shakya, S. Fan, and M. Lipson, *ibid.* **96**, 123901 (2006); K. Totsuka, N. Kobayashi, and M. Tomita, *ibid.* **98**, 213904 (2007).
[10] T. W. Ebbesen, C. Genet, and S. I. Bozhevolnyi, Phys. Today **61**, 44 (2008).
[11] S. Zhang, D. A. Genov, Y. Wang, M. Liu, and X. Zhang, Phys. Rev. Lett. **101**, 047401 (2008).
[12] P. Tassin, L. Zhang, T. Koschny, E. N. Economou, and C. M. Soukoulis, Phys. Rev. Lett. **102**, 053901 (2009); Opt. Express **17**, 5595 (2009); R. Singh, C. Rockstuhl, F. Lederer, and W. Zhang, Phys. Rev. B **79**, 085111 (2009); H. Xu and B. S. Ham, arXiv:0905.3102v4 (unpublished); Y. Lu, H. Xu, N. T. Tung, J. Y. Rhee, W. H. Jang, B. S. Ham, and Y. P. Lee, arXiv:0906.4029v2 (unpublished).
[13] N. Papasimakis, V. A. Fedotov, N. I. Zheludev, and S. L. Prosvirnin, Phys. Rev. Lett. **101**, 253903 (2008); N. Papasimakis, Y. H. Fu, V. A. Fedotov, S. L. Prosvirnin, D. P. Tsai, and N. I. Zheludev, Appl. Phys. Lett. **94**, 211902 (2009).
[14] S. Linden, J. Kuhl, and H. Giessen, Phys. Rev. Lett. **86**, 4688 (2001).
[15] A. Christ, S. G. Tikhodeev, N. A. Gippius, J. Kuhl, and H. Giessen, Phys. Rev. Lett. **91**, 183901 (2003); A. Christ, T. Zentgraf, J. Kuhl, S. G. Tikhodeev, N. A. Gippius, and H. Giessen, Phys. Rev. B **70**, 125113 (2004); A. Christ, Y. Ekinci, H. H. Solak, N. A. Gippius, S. G. Tikhodeev, and O. J. F. Martin, *ibid.* **76**, 201405(R) (2007).
[16] A. Sharon, D. Rosenblatt, and A. A. Friesem, J. Opt. Soc. Am. A Opt. Image Sci. Vis. **14**, 2985 (1997).
[17] G. Gantzounis, N. Stefanou, and V. Yannopapas, J. Phys.: Condens. Matter **17**, 1791 (2005).
[18] N. Stefanou, V. Yannopapas and A. Modinos, Comput. Phys. Commun. **113**, 49 (1998); Comput. Phys. Commun. **132**, 189 (2000).
[19] M. S. Bigelow, N. N. Lepeshkin, and R. W. Boyd, J. Phys.: Condens. Matter **16**, R1321 (2004).

[20] P. C. Ku, C. J. Chang-Hasnain, and S. L. Chuang, J. Phys. D **40**, R93 (2007).
[21] D. R. Smith, S. Schultz, P. Markoš, and C. M. Soukoulis, Phys. Rev. B **65**, 195104 (2002).
[22] C. Tserkezis, N. Papanikolaou, G. Gantzounis, and N. Stefanou, Phys. Rev. B **78**, 165114 (2008).
[23] S. Enoch, G. Tayeb, P. Sabouroux, N. Guérin, and P. Vincent, Phys. Rev. Lett. **89**, 213902 (2002).
[24] S. Tretyakov, I. Nefedov, A. Sihvola, S. Maslovski, and C. Simovski, J. Electromagn. Waves Appl. **17**, 695 (2003).
[25] R. W. Ziolkowski, Phys. Rev. E **70**, 046608 (2004).
[26] M. D. Lukin, S. F. Yelin, M. Fleischhauer, and M. O. Scully, Phys. Rev. A **60**, 3225 (1999); E. Paspalakis and P. L. Knight, *ibid.* **66**, 015802 (2002).
[27] J. L. Beeby, J. Phys. C **1**, 82 (1968).
[28] A. Gonis, *Green Functions for Ordered and Disordered Systems* (North Holland, Amsterdam, 1992).
[29] N. Stefanou and A. Modinos, J. Phys.: Condens. Matter **3**, 8135 (1991); **3**, 8149 (1991).
[30] V. Yannopapas, A. Modinos, and N. Stefanou, Phys. Rev. B **60**, 5359 (1999).
[31] V. Yannopapas, Phys. Rev. B **75**, 035112 (2007).
[32] V. Yannopapas, A. Modinos, and N. Stefanou, Opt. Quantum Electron. **34**, 227 (2002).
[33] R. B. Johnson and R. W. Christy, Phys. Rev. B **6**, 4370 (1972).
[34] C. Tserkezis, G. Gantzounis, and N. Stefanou, J. Phys.: Condens. Matter **20**, 075232 (2008).